LIMNOLOGY and OCEANOGRAPHY

ASLO

Limnol. Oceanogr. 9999, 2020, 1–14

doi: 10.1002/lno.11585

Plasticity in the grazing ecophysiology of *Florenciella* (Dichtyochophyceae), a mixotrophic nanoflagellate that consumes *Prochlorococcus* and other bacteria

Qian Li,[1,2] Kyle F. Edwards,[1] Christopher R. Schvarcz,[1,2] Karen E. Selph,[1] Grieg F. Steward [1,2]*

[1]Department of Oceanography, School of Ocean and Earth Science and Technology (SOEST), University of Hawai'i at Mānoa, Honolulu, Hawaii

[2]Center for Microbial Oceanography: Research and Education, School of Ocean and Earth Science and Technology (SOEST), University of Hawai'i at Mānoa, Honolulu, Hawaii

Abstract

Mixotrophic nanoflagellates can account for more than half of the bacterivory in the sunlit ocean, yet very little is known about their ecophysiology. Here, we characterize the grazing ecology of an open-ocean mixotroph in the genus *Florenciella* (class Dictyochophyceae). Members of this class were indirectly implicated as major consumers of *Prochlorococcus* and *Synechococcus* in the oligotrophic North Pacific Subtropical Gyre, but their phagotrophic capabilities have never been investigated. Our studies showed that *Florenciella* readily consumed *Prochlorococcus*, *Synechococcus*, and heterotrophic bacteria, and that the ingested prey relieved nutrient limitations on growth. *Florenciella* grew faster (3 d^{-1}) in nitrogen-deplete medium given sufficient live *Synechococcus*, than in nitrogen-replete K medium (2 d^{-1}), but it did not grow in continuous darkness. Grazing rates were substantially higher under nutrient limitation and showed a hint of diel variability, with rates tending to be highest near the end of the light period. An apparent trade-off between the maximum clearance rate (5 nL *Florenciella*$^{-1}$ h^{-1}) and the maximum ingestion rate (up to ~ 10 prey cells *Florenciella*$^{-1}$ h^{-1}) across experiments suggests that grazing behavior may also vary in response to prey concentration. If the observed grazing rates are representative of other open-ocean mixotrophs, their collective activity could account for a significant fraction of the daily cyanobacterial mortality. This study provides essential parameters for understanding the grazing ecology of a common marine mixotroph and the first characterization of mixotrophic nanoflagellate functional responses when feeding on unicellular cyanobacteria, the dominant marine primary producers in the oligotrophic ocean.

Mixotrophy, the combining of photosynthetic and phagotrophic nutrition, is a widespread strategy among protists (Sanders 1991; Jones 2000; Stoecker et al. 2017). By consuming prey, mixotrophs can thrive under conditions in which a strict autotroph would be limited by the availability of inorganic nutrients (Lindehoff et al. 2010) or light (McKie-Krisberg et al. 2014). At the same time, photosynthesis by mixotrophs can relieve energy limitation relative to strict heterotrophic grazers (Fischer et al. 2017). Mixotrophs are therefore expected to be successful under high-light, low-nutrient conditions in competition with autotrophs, but can also prosper under nutrient-rich conditions in competition with heterotrophs (Edwards 2019).

Evidence for the prevalence of mixotrophs and their importance in open-ocean ecosystems has been mounting for some time (Worden et al. 2015). On average, mixotrophic nanoflagellates are responsible for about half of bacterivory in experiments that compare them to heterotrophic nanoflagellates and contribute the majority of bacterivory at lower latitudes (Hartmann et al. 2012). Mixotrophic flagellates have also been shown to graze on cyanobacteria such as *Prochlorococcus* and *Synechococcus* (Sanders et al. 2000; Jeong et al. 2005), which are responsible for a large fraction of total photosynthesis in the open ocean (Partensky et al. 1999). *Prochlorococcus*, in particular, is the most abundant marine photoautotroph (Chisholm 2012), but remarkably little is known about the identity, physiology, or ecology of the grazers feeding on it. This makes it difficult to explain or model the mortality rates of the most common primary producer in the ocean.

*Correspondence: grieg@hawaii.edu

Additional Supporting Information may be found in the online version of this article.

One group of mixotrophs that has been implicated in consuming cyanobacteria is heterokont algae in the class Dictyochophyceae. Stable isotope probing at Station ALOHA in the North Pacific Subtropical Gyre (NPSG) suggested that dictyochophytes, and members of the genus *Florenciella* (Eikrem et al. 2004) in particular, were one of several groups grazing most actively on *Prochlorococcus* and *Synechococcus* (Frias-Lopez et al. 2009). Dictyochophytes have also been found to graze on bacteria in polar oceans (Gast et al. 2018), and they were identified as important grazers of heterotrophic bacteria and picocyanobacteria in two freshwater lakes (Gerea et al. 2019). Despite their apparent widespread contributions to grazing mortality, there have been no studies to characterize the grazing behavior of dictyochophytes. Indeed, there has been little quantitative work on any open ocean mixotrophic nanoflagellates, and none characterizing their feeding behavior on *Prochlorococcus*.

Laboratory studies of mixotroph functional responses or growth vs. prey density have thus far focused primarily on larger mixotrophs (Hansen 2011) or on nanoflagellates feeding on heterotrophic bacteria (Legrand et al. 2001). The few studies investigating nanoflagellate grazers of *Prochlorococcus* have focused on heterotrophs rather than mixotrophs (Christaki et al. 2002). As a consequence, we lack the data to parameterize a key part of the microbial loop in ecosystem models, to estimate the role of mixotrophic nanoflagellates in carbon and nutrient fluxes, and to assess the trade-offs that affect mixotrophic strategies as compared to autotrophy and heterotrophy. In this study, we help fill this major gap with the first characterization of the grazing ecophysiology of a strain of *Florenciella* isolated from the oligotrophic open ocean.

Materials and methods

Mixotroph and prey cultures

An isolate in the genus *Florenciella* (strain UA-265-01) was enriched in K medium (Keller et al. 1987) minus nitrogen (K-N) from water collected in the euphotic zone at Station ALOHA in the NPSG in September 2014. The isolate was rendered unialgal, but not axenic, and maintained at 24°C in K medium ($\sim$ 1000 μM N, $\sim$ 8 μM P), K-N ($\sim$ 0.2 μM N), or K minus phosphorus (K-P) ($\sim$ 0.2 μM P), under a 12 : 12 light : dark cycle. The light period ran from 07:00 to 19:00 h at an irradiance of $\sim$ 100 μmol photons m^{-2} s^{-1}. *Florenciella* maintained in nutrient-deplete medium had sufficient limiting nutrient for modest growth (yields of 10^3–10^4 cells mL^{-1}) but were occasionally fed with prey to acclimate them to grazing and generate sufficient biomass prior to grazing experiments. Cultures of cyanobacteria used as prey in our experiments—*Prochlorococcus* str. MIT9301 and *Synechococcus* str. WH8102—were axenic and maintained in Pro99 medium (Moore et al., 2007). Two heterotrophic bacteria used as experimental prey—a *Marinobacter* sp. (family *Alteromonadaceae*) and an unknown member of the family *Rhodobacteraceae*—were isolated from the *Florenciella* culture and grown in Difco Marine Broth 2216. Dimensions of *Florenciella* and prey cells were measured using transmitted light and epifluorescence microscopy, and the detailed morphology and ultrastructure of *Florenciella* was examined by scanning and transmission electron microscopy (Supplementary Methods). The phylogeny of the new *Florenciella* isolate and taxonomic identification of the bacterial isolates were inferred from small subunit rRNA partial gene sequences (Supplementary Methods), and the sequences were deposited in GenBank with accession numbers MN615711 (*Florenciella*), MN133870 (*Marinobacter*), and MN133871 (unknown *Rhodobacteraceae*). Elemental analysis of the media, *Florenciella*, and prey cells were conducted using standard analytical methods (Supplementary Methods).

Several different types of experiments, described in detail below, were conducted to investigate various aspects of the grazing functional ecology of *Florenciella* (Table 1). These included experiments to (1) confirm ingestion of prey (short-term prey uptake); (2) determine grazing rate (long-term prey disappearance) and how the rate is affected by nutrient limitation, time of day, as well as prey type and concentration; and (3) determine the effect of prey type and concentration on *Florenciella* growth rate.

Detecting prey ingestion

Short-term incubations ($\leq$ 1 h) were carried out to detect relative rates of prey ingestion. Live, unstained *Synechococcus*, live, stained *Prochlorococcus* (Hoechst 33342 or SYBR Green I; Thermo Fisher), or fluorescent beads (0.5 or 1.0 μm Fluoresbrite Microspheres; Polysciences) were added in triplicate to *Florenciella* cultures at final concentrations of 10^5–10^6 mL^{-1}. For negative controls, *Florenciella* was treated with cytochalasin B (Sigma-Aldrich; 10 μg mL^{-1} final concentration) for 1–2 h prior to adding prey to inhibit phagocytosis (Leakey et al. 1994). *Florenciella* that had ingested prey were identified by flow cytometry (Attune NxT; Thermo Fisher Scientific) as those cells having the same chlorophyll fluorescence and light scattering signature as *Florenciella*, but which had also acquired the characteristic prey fluorescence. Samples were collected at short time intervals (0, 5, 10, 20, and 40 min) and fixed with an equal volume of ice-cold glutaraldehyde (2% final concentration) to prevent vacuole ejection (Caron 2001). Pluronic F-68 (Sigma Aldrich) was added to fixed samples (0.01% final concentration) to minimize clumping (Marie et al. 2014).

Florenciella that had been incubated with *Synechococcus* were examined using laser confocal microscopy (TCS SP8 X; Leica Microsystems) to obtain visual evidence of prey ingestion. Cells were first stained with CellBrite Fix 488 Membrane Stain (Biotium), and then fixed with alkaline Lugol's solution (0.5% final concentration) followed immediately with borate-buffered formaldehyde (2% final concentration; Sherr et al. 1987). Color from iodine in the Lugol's was cleared with a few drops of sodium thiosulfate, and fixed cells were then stained with the blue fluorescent DNA stain 4′,6-diamidino-2-phenylindole,

Table 1. Summary of experiments used to evaluate grazing ecology and growth of a mixotrophic *Florenciella* (Flo) isolate (strain UA-265-01).

Experiment	Conditions (medium)	Incubation time	Sampling interval	Process targeted	Measurement (tool)	Analysis
Ingestion	Single prey (K-N)	40 min–1 h	5–20 min	Confirming prey ingestion Relative short-term uptake	Visual (confocal microscopy) % Flo associated with prey (flow cytometry)	Short-term prey uptake/ ingestion
	Single prey (K, K-N, or K-P)	3–7 d	2–24 h	Nutrient effects on grazing	Prey and Flo abundance over time (flow cytometry)	Prey disappearance in K-N vs. K medium
Grazing rates	Single prey (K-N)	5 h–7 d	2–24 h	Flo grazing rate		Ingestion and clearance rate (prey disappearance)
				Grazing functional responses	Prey and Flo abundance over time (flow cytometry)	Maximum ingestion and clearance rate (dynamic model fit)
				Diel rhythmicity of grazing		Ingestion rate at different times of day (generalized additive mixed model)
	Multiple prey (K-N)	5 h–7 d	2–12 h	Prey preference	Prey and Flo abundance over time (flow cytometry)	Relative clearance rates among prey
				Diel rhythmicity of grazing		Ingestion rate of all prey at different times of day
Growth rates	Single prey (K-N) No added prey (K)	5 d	~0.5 d	Effect of prey type and concentration on Flo growth rate	Flo abundance over time (flow cytometry)	Specific growth rate (nonlinear curve fit)

dihydrochloride (DAPI; Biotium) and collected on 3.0 μm pore size polycarbonate membrane filters (Whatman). Filters were mounted in glycerol-based antifade mountant (SlowFade Diamond; Thermo Fisher) and scanned with illumination settings for DAPI (Ex. 405 nm, Em. 400–480 nm), chlorophyll (Ex. 450 nm, Em. 640–700 nm), CellBrite (Ex. 488 nm, Em. 500–550 nm), and phycoerythrin (Ex. 545 nm, Em. 550–620 nm).

Grazing experiments and functional responses

Longer term grazing experiments (from 5 h to 1 week in duration) were conducted to quantify ingestion and clearance rates based on rates of prey disappearance. Live, unstained prey cells were used for our grazing rate measurements to avoid the issue of negative discrimination of surrogate prey during ingestion, which could be problematic especially for mixotrophic flagellates (Weisse et al. 2016). Experiments were conducted in nutrient-replete, full K medium and nutrient-deplete (K-N or K-P) media to determine the effects of nutrients, prey type, and prey concentration on grazing. To minimize carryover of dissolved nutrients and prey division, *Prochlorococcus* and *Synechococcus* were first grown to stationary phase in the experimental medium, followed by pelleting ($2000 \times g$ for 3–5 min) and resuspension in fresh experimental medium. The heterotrophic bacteria were simply pelleted and resuspended twice in the experimental medium. Minimal nutrient carryover was confirmed by nutrient analysis.

Concentrated prey were added to a newly transferred *Florenciella* culture (initial concentration of 10^3–10^4 cells mL^{-1} with 10^4–10^5 cells mL^{-1} ambient bacteria) at final concentrations of 10^5–10^8 prey cells mL^{-1} (different dilution ratios were implemented to make sure amended prey was > 10 times the ambient bacteria). Cell concentrations of prey and *Florenciella* were determined by flow cytometry analysis of glutaraldehyde-fixed samples collected at intervals varying from 2 to 24 h. Populations were distinguished based on light scatter and either pigment autofluorescence (*Florenciella*, *Synechococcus*, *Prochlorococcus*) or DNA fluorescence (heterotrophic bacteria, stained post-sampling with SYBR Green I). In the grazer-free negative control, prey were added into an equal volume of cell-free filtrate (< 0.22 μm) from the same *Florenciella* culture to test for growth of the prey that would result in underestimates of prey ingestion. Individual treatments were not replicated within an experiment, but the entire grazing experiment comparing grazing in K vs. K-N was repeated and an additional experiment in K-P was conducted for comparison. In addition, a total of 12 (*Prochlorococcus*), 11 (*Synechococcus*),

and 3 (*Marinobacter*) single-prey grazing experiments were carried out in K-N medium at a wide range of initial prey concentrations to estimate grazing rates and functional responses.

We calculated ingestion rates, I (prey cell^{-1} h^{-1}) for *Florenciella* as:

$$I = \frac{\text{Prey}_\text{i} - \text{Prey}_\text{f}}{\textit{Florenciella}_\text{avg}(t_\text{f} - t_\text{i})} \quad (1)$$

where Prey_i and Prey_f are the initial and final abundance of prey (prey mL^{-1}), $\textit{Florenciella}_\text{avg}$ is the arithmetic mean abundance of *Florenciella* (cells mL^{-1}) over the time interval, and t_f and t_i are the final and initial sampling times (h) for the interval. The clearance rate (C, nL cell^{-1} h^{-1}) was calculated by dividing the ingestion rate by average prey concentration over the same interval.

For the grazing functional responses, we assumed that the decline of the prey population due to grazing could be represented by the equation:

$$\frac{\text{d}P}{\text{dt}} = -Fg(P) \quad (2)$$

where P is the prey concentration at time t, F is *Florenciella* concentration at time t, and $g(P)$ is the functional response of *Florenciella*. For $g(P)$, we used the hyperbolic tangent (tanh) rather than the more common Holling type 2 curve (Sandhu et al. 2019), because preliminary analysis showed that hyperbolic tangent fit as well or better and yielded more reasonable estimates of the maximum ingestion rate. The hyperbolic tangent functional response is $g(P) = I_\text{max}\tanh\left(P\frac{C_{max}}{I_{max}}\right)$, where I_max is the maximum ingestion rate and C_max is the maximum clearance rate. Equation 2 assumes that the prey population does not grow during the experiment. In experiments with heterotrophic bacteria, the prey did grow, therefore the functional response parameters for grazing on these bacteria are conservative estimates. Equation 2 was fit to trajectories of prey and grazer abundances using maximum likelihood. Grazer abundance was interpolated throughout the entire interval using the fitted smoother from a generalized additive model (Wood 2011). The differential equation was then solved numerically with the package deSolve in R (Soetaert et al. 2010), and maximum likelihood parameters were found by optimization with bbmle (Bolker et al. 2017). The fitted parameters were I_max, C_max, the measurement error variance (lognormal distribution), and the initial prey abundance used to initialize the solution of the ordinary differential equation.

Nineteen additional multiple-prey experiments using mixtures of two or three prey types among *Prochlorococcus*, *Synechococcus*, and two heterotrophic bacteria, were performed in K-N medium to investigate prey preferences. Within an experiment, multiple estimates of clearance rate for each prey were calculated from changes in abundance over each time interval during the incubation. To allow easier comparison of relative prey preferences among experiments, the clearance rates for each prey within an experiment were normalized to the average rate for the prey with the fastest mean clearance rate in that experiment. An average (± SE) relative clearance rate was calculated from all of the individual normalized rate estimates within and across all experiments conducted with the same combination of prey.

Potential diel patterns in *Florenciella* grazing rate were analyzed by compiling rate data from discrete intervals (2–12 h) from both single- and multiple-prey experiments. In the latter case, the ingestion rate was taken as the total for all added prey. Ingestion rate was used as the response variable in a generalized additive mixed model (R package gamm4; Wood and Fabian 2017), where the predictors included a smoother for log[total prey], a smoother for time of day (the midpoint of the sampling interval), a random effect for experiment (to account for the fact that grazing rate may be higher on average in some experiments), and a random effect for prey type.

Florenciella growth rate experiment

Exponential growth rates of *Florenciella* as a function of prey type (*Prochlorococcus*, *Synechococcus*, or *Marinobacter*) and concentration were measured in batch culture, with a *Florenciella* starting concentration of $\sim 1 \times 10^3$ cells mL^{-1}. Concentrated prey stocks were added into triplicate incubations twice per day to maintain concentrations close to the indicated nominal target prey concentration (5×10^5, 10^6, 5×10^6, and 10^7 cells mL^{-1}). Exponential growth rate at each target prey concentration was estimated by fitting a nonlinear growth curve that includes a lag period (if present) and a carrying capacity (Ward et al. 2017). This approach has the advantage of fitting all of the data, rather than only the points subjectively determined to fall in the log-linear phase. To verify the suitability of the nonlinear model, we compared growth rates using that approach with the common technique of linear regression through the linear portion of a plot of ln [cell] vs. time, with the exponential growth phase judged by eye.

Cellular stoichiometry and nutrient assimilation efficiency

An apparent nitrogen assimilation efficiency for *Florenciella* when prey were the primary source of nitrogen (K-N medium) was calculated as:

$$E = \frac{(F_\text{fp} - F_\text{fc})}{(p_\text{i} - p_\text{f})}\left(\frac{\text{QF}}{\text{Qp}}\right) \quad (3)$$

where F_fp and F_fc are the *Florenciella* final concentrations in samples with prey or in controls with no added prey, p_i and p_f are initial and final prey concentrations in the grazing cultures, and Q_F and Q_p are the cellular N quotas of *Florenciella* or prey.

Results

Morphology and phylogeny of *Florenciella*

Cells were approximately spherical, between 3 and 6 μm in diameter (4 $\pm$ 0.7 μm, average $\pm$ SD, n = 86), and bore two flagella of unequal length (Supplementary Fig. S1a,b). Thin sections revealed two chloroplasts, mitochondria, flagella, and apparent food vacuoles (Supplementary Fig. S1c–f). The 18S rRNA gene sequence of *Florenciella* strain UA-265-01 had 97.4% similarity to the first described *Florenciella* isolate (*Florenciella parvula*; Eikrem et al. 2004) and clustered with environmental sequences from the Pacific Ocean and with the sequences from *Florenciella* strains previously isolated from the Atlantic and Pacific Oceans (Supplementary Fig. S2).

Detection of prey ingestion

Prey were directly observed within *Florenciella* cells by confocal microscopy within 1 h of initiating grazing experiments (Fig. 1). The percentage of *Florenciella* associated with fluorescent prey, as determined by flow cytometry (Supplementary Fig. S3), generally began increasing within 10 min and plateaued within 20 to 40 min (Fig. 2). The maximum percentage varied depending on prey concentration and prey type. At a prey concentration of $\sim 10^6$ cells mL^{-1}, *Florenciella* with detectable prey reached 23 ($\pm$ 4) % or 35 ($\pm$ 2) % on average ($\pm$ SD) when feeding on *Prochlorococcus* or *Synechococcus*, respectively. No discernible uptake was observed when *Florenciella* was treated with cytochalasin B. The uptake of microspheres at a similar concentration was slower and saturating percentages were lower, that is, 6 ($\pm$ 1) % and 12 ($\pm$ 2) % on average ($\pm$ SD) for 0.5 and 1.0 μm beads, respectively.

Effect of nutrient limitation on grazing behavior

In experiments using full K medium, *Prochlorococcus* and *Synechococcus* added at a concentration of 2×10^6 cells mL^{-1}

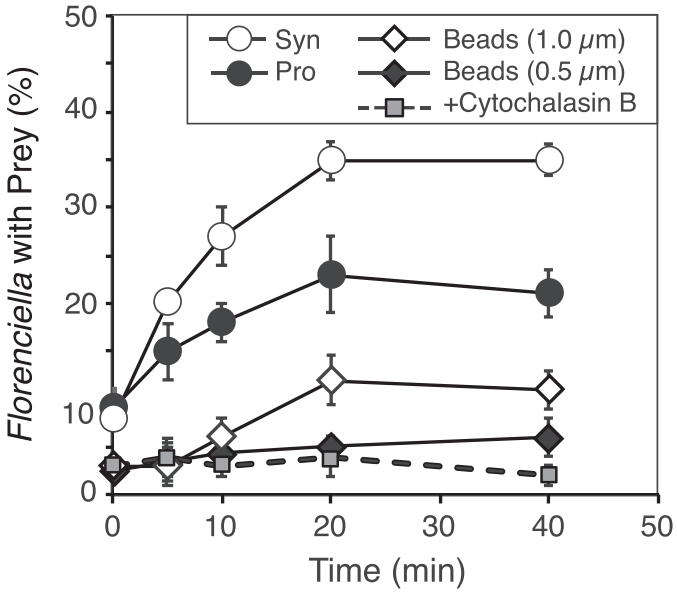

Fig. 2. Association of prey with *Florenciella* detected by flow cytometry. The percentage of *Florenciella* cells associated with each of four prey (average $\pm$ SD; n = 3) are shown as a function of time with similar starting prey concentrations: *Prochlorococcus* (Pro, 9×10^5 cells mL^{-1}), *Synechococcus* (Syn, 1.0×10^6 cells mL^{-1}), and microspheres (0.5 and 1.0 μm, 8×10^5 and 6×10^5 beads mL^{-1}, respectively). Points for the cytochalasin B-treated negative control are averages ($\pm$ SD; n = 3) of the results for the single treatments in each of the Pro, Syn, and beads experiments.

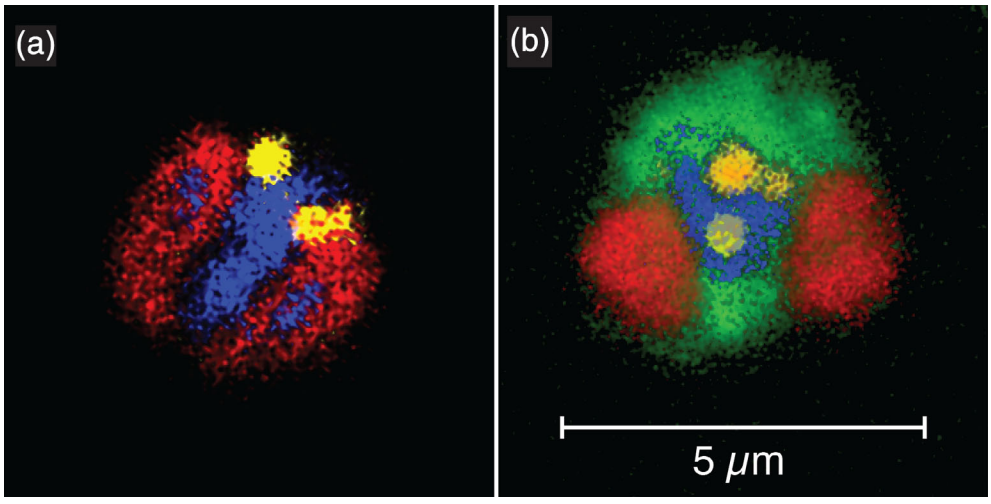

Fig. 1. *Florenciella* with ingested *Synechococcus* imaged in z-slices of two different cells by laser scanning confocal microscopy. Fixed cells were stained with the DNA stain 4′,6-diamidino-2-phenylindole, dihydrochloride (DAPI) (**a**) or with DAPI and CellBrite fix (**b**). *Florenciella* chloroplasts are seen in red (chlorophyll autofluorescence), the nucleus in blue (DAPI), and membrane in green (CellBrite fix). *Synechococcus* are yellow (phycoerythrin autofluorescence).

increased slightly (< 1 doubling) over the first 24 to 48 h (Fig. 3a,c). Over this period, there was no discernible difference in growth rate of the prey in the presence or absence of *Florenciella*, nor was there a discernible difference in initial exponential growth rate of *Florenciella* in the presence or absence of prey (Fig. 3b,d). After the initial increase, prey cells remained relatively stable in the absence of *Florenciella*. In the presence of *Florenciella*, prey concentrations declined slowly over 5–7 d but never dropped below the initial concentration. The final yields of *Florenciella* in K medium were similar with or without added prey, but they were slightly higher (5–10%) when prey was added (Fig. 3b,d).

In contrast, *Prochlorococcus* and *Synechococcus* added to K-N medium were stable in the absence of *Florenciella*, but declined in the presence of *Florenciella* by an order of magnitude over 6 d (*Prochlorococcus*; Fig. 3a) or by several orders of magnitude in only 2–3 d (*Synechococcus*; Fig. 3c). These rates of removal were about an order of magnitude faster than observed in K medium despite there being, in the experiment with *Prochlorococcus*, lower concentrations of *Florenciella* for the duration of the experiment. In K-N medium, the addition of prey substantially increased both the yield and growth rate of *Florenciella*, with the stimulation being more pronounced for *Synechococcus* (Fig. 3d) than *Prochlorococcus* (Fig. 3b). This is consistent with the faster and more complete removal of *Synechococcus* relative to *Prochlorococcus* under these conditions. A similar effect of nutrient limitation on prey disappearance and *Florenciella* growth rate was seen in a second set of experiments with different starting *Synechococcus* and *Prochlorococcus* concentrations (Supplementary Fig. S4) suggesting that this nutrient effect is eproducible. *Synechococcus* and *Prochlorococcus* were also grazed in the presence of *Florenciella* when phosphorus rather than nitrogen was the limiting nutrient (Supplementary Fig. S5).

The concentrations of *Marinobacter* increased 10- to 20-fold when added to full K medium. In contrast to the situation with

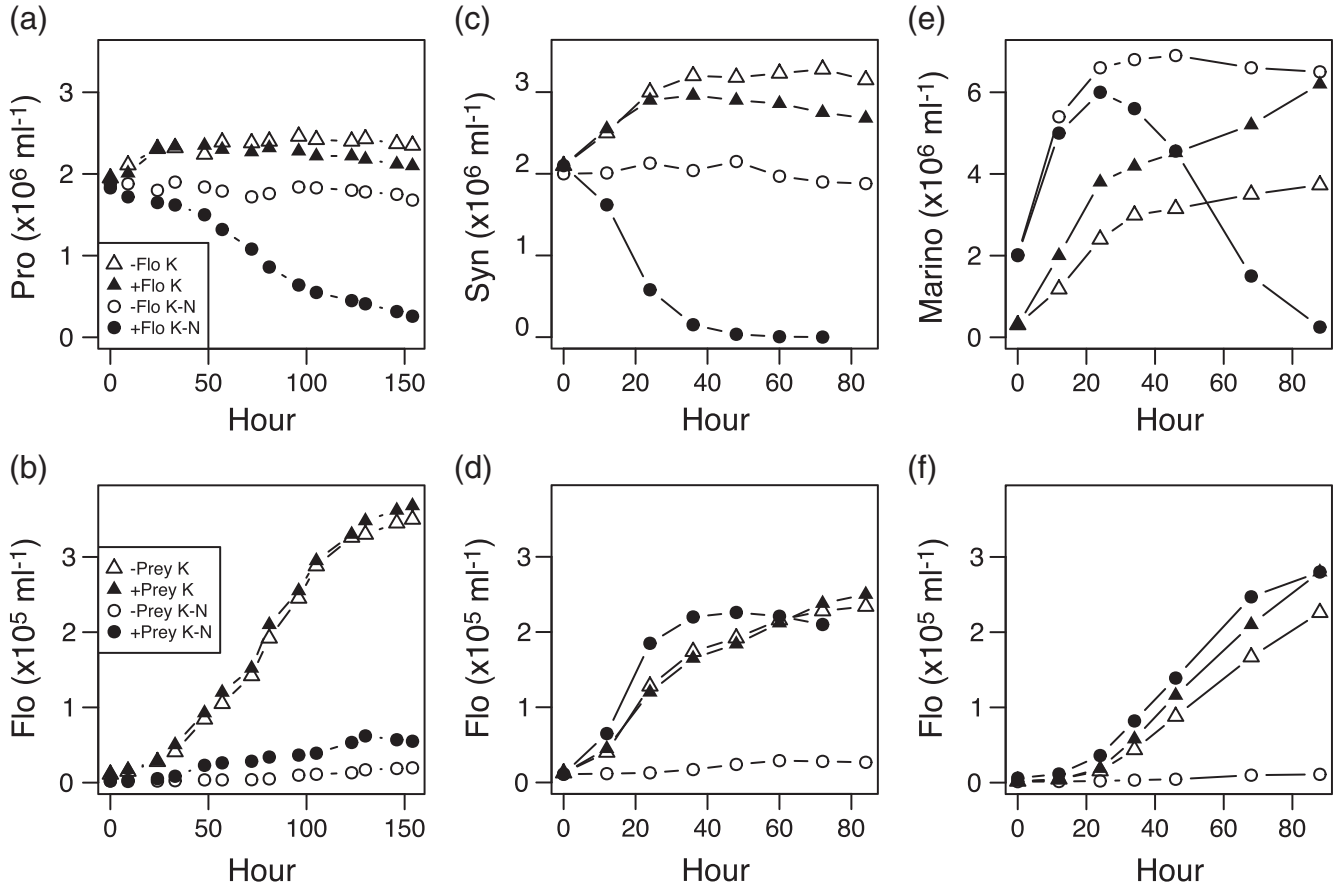

Fig. 3. Prey and *Florenciella* (Flo) dynamics during representative grazing experiments under N-replete and N-deplete conditions. Prey used were *Prochlorococcus* (Pro; **a**, **b**), *Synechococcus* (Syn; **c**, **d**), or *Marinobacter* (Marino; **e**, **f**). Prey concentrations are shown over time in full K or K-N medium, in the presence or absence of *Florenciella* (**a**, **c**, **e**). *Florenciella* concentrations are shown over time in full K or K-N medium, with or without added prey (**b**, **d**, **f**). Ambient bacteria concentrations (< 2×10^5 cells mL^{-1} throughout the experiments) were low in *Florenciella* culture grown in K-N medium relative to added prey and supported minimal *Florenciella* growth (yields of only $\sim 1 \times 10^4$ cells mL^{-1}) among all controls (–prey in K-N; panels **b**, **d**, **f**). Individual treatments shown in these plots are not replicated, but the experiments illustrated in panels (**a**–**d**) were repeated, but with approximately half the starting prey concentration, and showed the same results (Supplementary Fig. S4).

Prochlorococcus and *Synechococcus*, *Marinobacter* concentrations increased more in the presence than in the absence of *Florenciella* (Fig. 3e). In K-N medium, *Marinobacter* increased 2.5-fold over the first 24 h in the presence or absence of *Florenciella* (Fig. 3e). The concentration then remained steady in the absence of *Florenciella*, but was reduced by 24-fold over the ensuing 2.8 d in the presence of *Florenciella*. *Florenciella* grew similarly well in the presence of *Marinobacter* regardless of medium, but grew somewhat slower in K in the absence of added *Marinobacter* (Fig. 3f). Growth of *Florenciella* was generally poor in K-N in the absence of added prey of any type (Fig. 3b,d,f).

Prey-supported *Florenciella* growth rate

Comparison of the nonlinear and log-linear regression models to estimate *Florenciella* growth rates (Supplementary Fig. S6) showed that the rates derived from the two models were similar on average and strongly correlated (r = 0.96, n = 40; Supplementary Fig. S7). However, because the estimates from the nonlinear model used all of the data, they were more precise (lower standard error) and not dependent on subjective choices of which points to model. Therefore, all growth rate data reported here derive from the nonlinear model fits. Growth rate of *Florenciella* in K-N, and its yield after 5 days of growth, varied as a function of prey type and concentration, and the rate showed a tendency toward saturation at the highest prey concentrations (Fig. 4). At a given cell concentration, *Florenciella* grew fastest on *Synechococcus*, followed by *Marinobacter*, then *Prochlorococcus*. The maximum growth rate of *Florenciella* when fed *Prochlorococcus* in K-N was 1.9 d^{-1} (Fig. 4). These rates are similar to the fastest growth observed when feeding on *Marinobacter* and slightly lower than growth in K medium with no added prey. The highest growth rate (3.2 d^{-1}) occurred when *Florenciella* was fed *Synechococcus* in K-N at an average sustained concentration of > 5×10^6 cells mL^{-1} (Fig. 4). This exceeded the growth rate of *Florenciella* grown in full K medium (2.2 d^{-1}). *Florenciella* was not able to grow in continuous darkness, regardless of the nutritional conditions (data not shown).

Elemental analysis indicated average (± SD) quotas of 475 (± 95) fg N per *Florenciella* cell, 15 (± 5) fg N per *Prochlorococcus*, 60 (± 14) fg N per *Synechococcus*, and 40 (± 1) fg N per *Marinobacter*. Combining these numbers with measurements of prey removal and *Florenciella* growth (Fig. 3; Supplementary Fig. S4) suggests N assimilation efficiencies for *Florenciella* grazing in K-N were high when feeding on any prey type, that is, averages (± SD) of 86 (± 9) % for *Prochlorococcus*, 68 (± 20) % for *Synechococcus*, and 67 (± 16) % for *Marinobacter*.

Functional response estimates

Across all experiments, C_{max} for *Florenciella* ranged from ~ 0.1 to 1.75 nL $cell^{-1}$ h^{-1} with *Prochlorococcus*, 0.05 to 5 nL $cell^{-1}$ h^{-1} with *Synechococcus*, and 0.2 to 0.55 nL $cell^{-1}$ h^{-1} with *Marinobacter* as the added prey. I_{max} ranged from 1 to 12, 0.1 to 16, and 2 to 3 prey $cell^{-1}$ h^{-1} for *Prochlorococcus*, *Synechococcus*, and *Marinobacter*, respectively (Fig. 5a–c; experiments in Supplementary Figs. S8–S10). In general, the grazing parameters varied more for *Synechococcus* than *Prochlorococcus*, and for both taxa, I_{max} and C_{max} tend to be negatively correlated across experiments (Fig. 5a; *Prochlorococcus* r = –0.55,

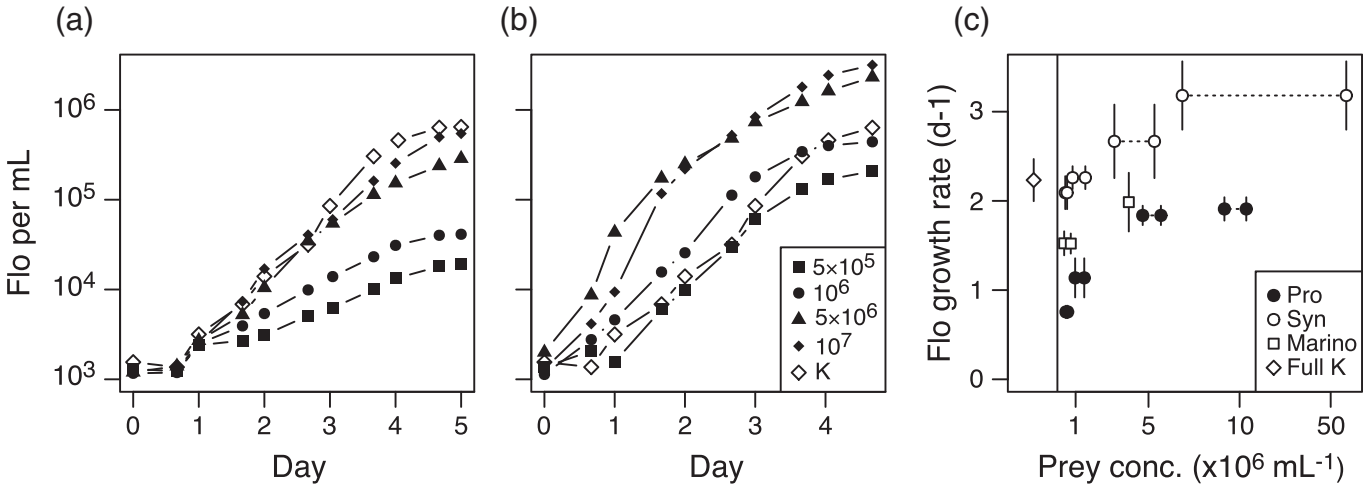

Fig. 4. Effect of prey type and concentration on *Florenciella* growth. *Florenciella* concentration is shown as a function of time when grown in K medium or in K-N medium in the presence of various concentrations of *Prochlorococcus* (Pro) (**a**) and *Synechococcus* (Syn) (**b**). All treatments conducted in triplicate (error bars not shown for clarity). Similar data for *Marinobacter* not shown. Exponential growth rates (average ± SE, n = 3) estimated from the curves in (**a**) and (**b**) and for *Marinobacter* are presented as a function of prey concentration for each prey type (**c**). In some experiments with Pro or Syn added as prey, growth of ambient bacteria was significant creating uncertainty about total available prey contributing to growth. To reflect this, each growth rate with Pro or Syn as prey is plotted twice (points connected by dotted lines). For each pair, the left point is at the observed average added prey concentration of Pro or Syn, and the right-hand point is at the total potential prey concentration including ambient bacteria.

p = 0.06; *Synechococcus* r = –0.72, p = 0.01). The variation in the parameters is also correlated with the initial prey density added during the experimental incubations. I_{max} tends to be greater when initial prey density is greater (Fig. 5b; *Prochlorococcus* r = 0.66, p = 0.02; *Synechococcus* r = 0.47, p = 0.14), while C_{max} tend to be lower when initial prey density is greater (Fig. 5c; *Prochlorococcus* r = –0.83, p = 0.001; *Synechococcus* r = –0.76, p = 0.007). In light of this variation in grazing parameters, we plotted typical functional responses under low prey density (10^5 cells mL^{-1}) and high prey density (10^7 cells mL^{-1}; Fig. 5d, e). Because I_{max} and C_{max} appear to acclimate to prey density, the acclimated ingestion rate under relatively constant conditions may be best predicted using the upper envelope of the "instantaneous" functional responses determined by a trade-off between I_{max} and C_{max} (Fig. 5f).

The estimates of C_{max} are likely more reliable than estimates of I_{max}, because the fitted functional responses were not strongly saturated over the range of prey densities used in all experiments (Supplementary Fig. S11). In particular, consumption of *Synechococcus* was more likely to exhibit substantial saturation than *Prochlorococcus*. However, because prey concentrations are relatively low in most oceanic environments, and especially in oligotrophic environments, C_{max} is more informative for quantifying grazing efficiency.

Grazing on multiple prey types

Prochlorococcus, *Synechococcus*, and *Marinobacter* are coccoid or nearly coccoid and have average (± SD, n = 20) cell diameters of 0.64 (± 0.10), 1.22 (± 0.23), and 0.84 (± 0.20) μm, respectively, but the *Rhodobacteraceae* isolate is rod shaped with an average length × width of 1.4 (± 0.29) × 0.4 (± 0.09) μm (Supplementary Fig. S12). Relative clearance rates when *Florenciella* were fed multiple prey types (Fig. 6; Supplementary Fig. S13) revealed: (1) higher clearance rate on *Synechococcus*

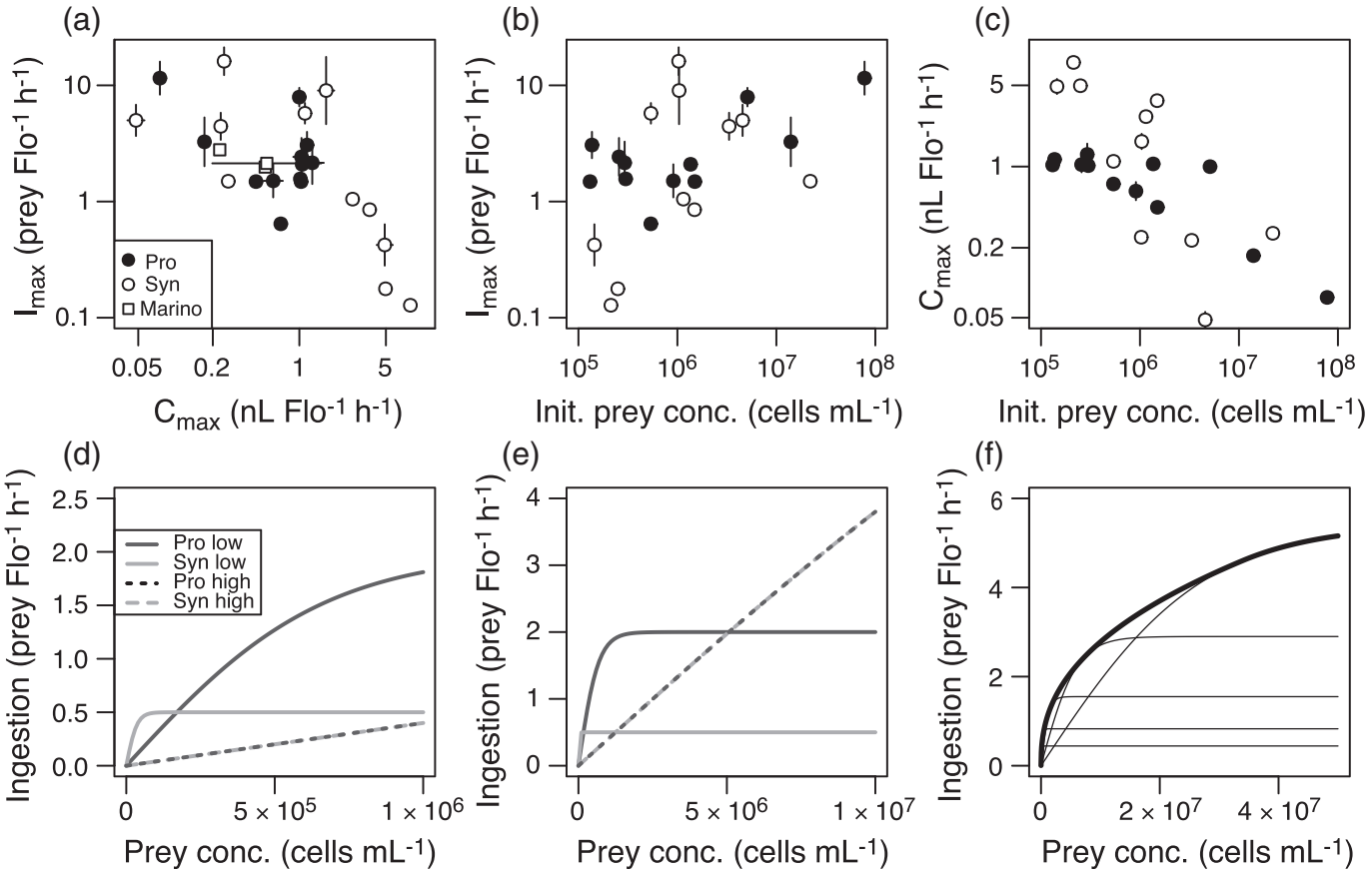

Fig. 5. *Florenciella* (Flo) grazing functional response estimates. (**a**) Estimated I_{max} plotted as a function of estimated C_{max} from experiments using *Prochlorococcus* (Pro), *Synechococcus* (Syn), or *Marinobacter* (Marino) as the added prey. (**b**) Variation in I_{max} as a function of the initial prey concentration. (**c**) Variation in C_{max} as a function of the initial prey concentration. (**d**) Typical functional response curves for Flo consuming Pro or Syn at initial prey densities of 10^5 mL^{-1} (low) or 10^7 mL^{-1} (high). (**e**) Same as (**d**) but with a wider range of prey concentrations on the x-axis. (**f**) Idealized "acclimated" vs. "instantaneous" functional responses of Flo when consuming Syn. Thin lines show how the instantaneous functional response varies as Flo is acclimated to different prey densities, assuming a trade-off between C_{max} and I_{max} that is derived by fitting a regression to the data in panel (**a**). The thick black line shows the numerically calculated upper envelope of the instantaneous curves, which is the predicted ingestion rate under constant prey densities. Error bars in (**a**–**c**) are standard errors of the parameter estimates. When error bars are not visible they are smaller than the symbols.

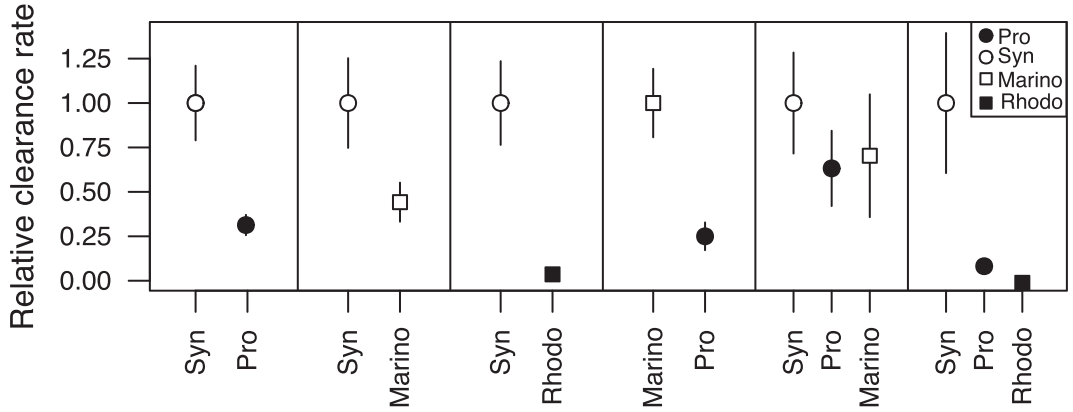

Fig. 6. Relative clearance rates of *Florenciella* (Flo) feeding on different combinations of *Prochlorococcus* (Pro), *Synechococcus* (Syn), *Marinobacter* (Marino) and unknown *Rhodobacteraceae* (Rhodo). Relative clearance rates are expressed as a fraction of the highest mean clearance rate within a given experiment. The average clearance rates (± SE) were calculated by pooling all rate estimates from within an experiment (calculated from different time intervals) and from all experiments with the same prey combination. The number of experiments (n_{expt}) and total number of clearance rate estimates (n_{rate}) for each prey in a given prey combination was: Syn + Pro (n_{expt} = 3, n_{rate} = 16), Syn + Marino (n_{expt} = 4, n_{rate} = 19), Syn + Rhodo (n_{expt} = 2, n_{rate} = 8), Marino + Pro (n_{expt} = 4, n_{rate} = 17), Syn + Pro + Marino (n_{expt} = 5, n_{rate} = 22), and Syn + Pro + Rhodo (n_{expt} = 1, n_{rate} = 4). All multiple prey experiments are shown in Supplementary Fig. S13.

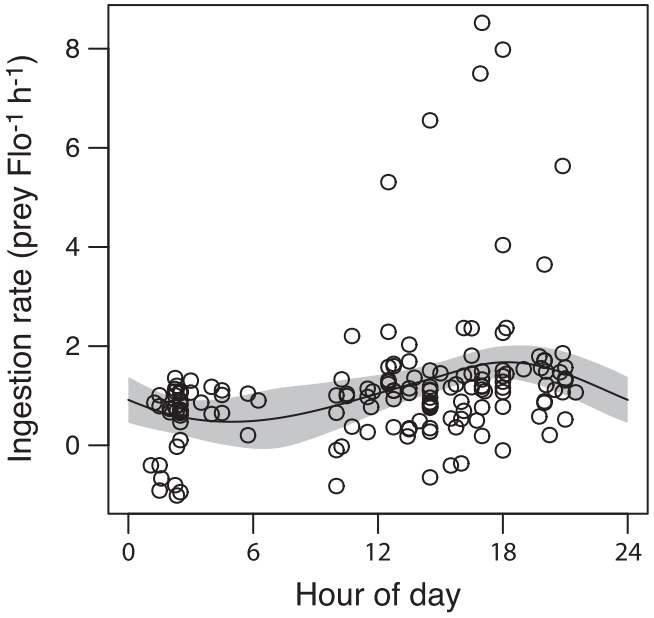

Fig. 7. Diel variation in *Florenciella* (Flo) ingestion rate. A smoother for time of day (midpoint of the sampling interval) from a generalized additive mixed model is plotted. The plotted ingestion rates are corrected for total prey density, such that the rate is that which would be expected if prey were at the average concentration in the dataset (1.8×10^6 cells mL^{-1}). The analysis combines experiments using different prey types as well as multiple prey types. Shaded area indicates 95% confidence level.

than *Prochlorococcus*, (2) *Marinobacter* appears intermediate between *Prochlorococcus* and *Synechococcus*, and (3) the *Rhodobacteraceae* cells are either not ingested or ingested at a very low rate, a conclusion supported by the failure of *Florenciella* to grow when fed this *Rhodobacteraceae* isolate in K-N (data not shown).

Diel variation in ingestion rate

According to a generalized additive mixed model, time of day explained significant variation in *Florenciella* ingestion rate (Fig. 7; partial R^2 = 0.06, $p < 0.001$) despite overall high variability. On average, ingestion peaked ~ 18:00 h and displayed a minimum ~ 06:00 h, with a 2- to 3-fold difference between these periods.

Discussion

With this study, we provide the first direct evidence of mixotrophy in the genus *Florenciella* and the first characterization of the functional response of a mixotroph grazing on *Prochlorococcus*. The first *Florenciella* strain isolated and described was not identified as a mixotroph (Eikrem et al. 2004), but stable isotope probing with labeled prey (Frias-Lopez et al. 2009) suggested that at least some members of this genus could be significant grazers of marine cyanobacteria in the wild. It may be that some species in the genus are not mixotrophic, but the use of K-N medium during isolation of the strain used in this study would have favored an isolate having this trait.

Grazing and growth ability of *Florenciella* relative to other nanoflagellates

Although grazing data for mixotrophic nanoflagellates are scant (and nonexistent for cyanobacteria as prey), *Florenciella* appears to have maximum clearance rates comparable to other mixotrophs (such as *Ochromonas*) but lower than heterotrophs (Fig. 8; Supplementary Table S1), which is consistent with the expectation that mixotrophs are constrained in their grazing performance by trade-offs with other functions such as photosynthesis and nutrient uptake. The generalist strategy of mixotrophy may also have selected for flexible fine-tuning of physiological processes, as the grazing behavior of *Florenciella*

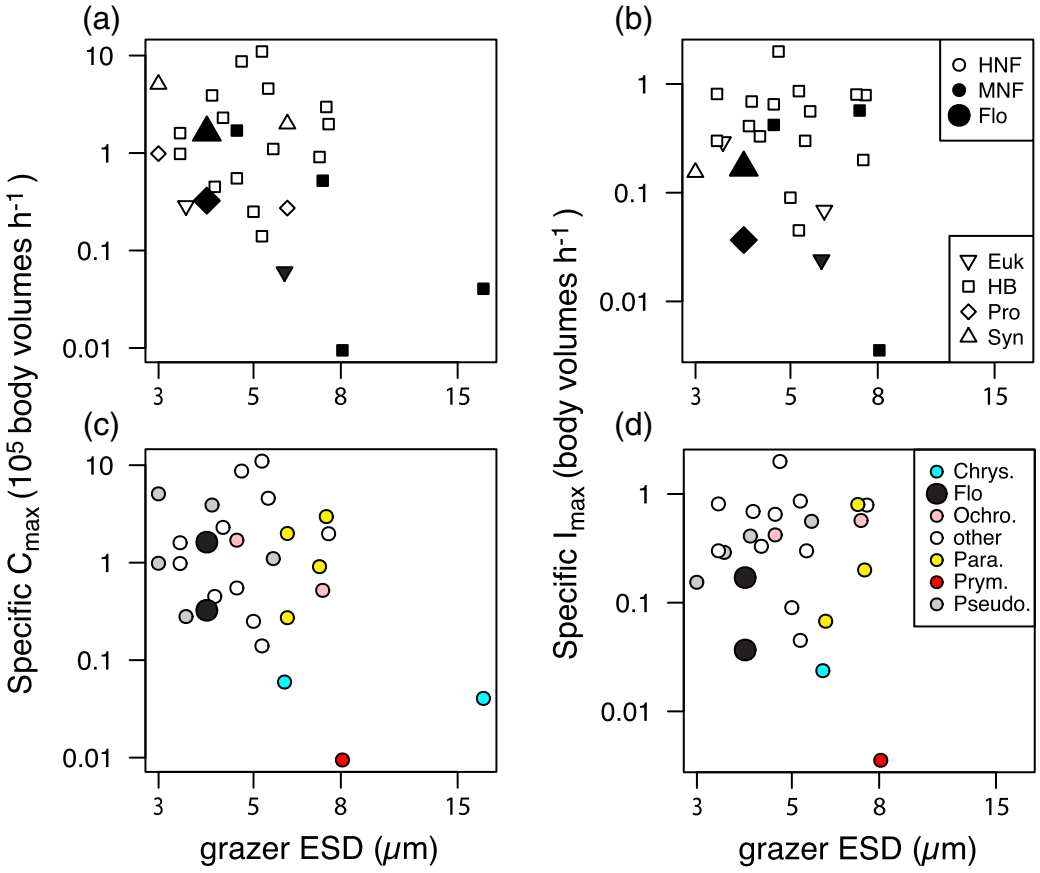

Fig. 8. Ingestion rate parameters as a function of size (equivalent spherical diameter, or ESD) for heterotrophic (HNF) and mixotrophic (MNF) nanoflagellates that have been studied in culture, as compared to our *Florenciella* (Flo) isolate. (**a**) Specific C_{max} (volume cleared per flagellate body volume per hour) or (**b**) specific I_{max} (prey volume ingested per flagellate body volume per hour) for flagellates grazing on *Prochlorococcus* (Pro), *Synechococcus* (Syn), heterotrophic bacteria (HB) or eukaryotic prey (Euk). In top panels (**a**, **b**), open symbols indicate HNF grazers, small closed symbols indicate MNF grazers, and large closed symbols indicate Flo as the grazer, symbol shapes indicate the type of prey (legend in panel b). (**c**–**d**) Same data as (**a**–**b**), but with points color coded according to grazer taxonomic affiliation (legend in panel d) including MNF in the genera *Chrysochromulina* (Chrys.), *Ochromonas* (Ochro.), *Prymnesium* (Prym.), and HNF *Paraphysomonas* (Para.), *Pseudobodo* (Pseudo.) and a variety of others (source data in Supplementary Table S1).

was sensitive to both nutrient concentration and prey concentration, as well as time of day. Although *Florenciella* may have lower clearance or ingestion rates than heterotrophic flagellates of similar size, mixotrophy may allow them to suppress prey densities to an equal or lower level, making them comparable or superior competitors. This can occur because energy and fixed C from photosynthesis subsidizes growth, relative to pure heterotrophs that tend to be energy-limited (Fischer, 2017; Edwards, 2019).

The maximum growth rate we observed for *Florenciella* under primarily autotrophic conditions (2.2 d^{-1} in K medium with no added prey) is relatively high, but not uncommon for phytoplankton (Thomas et al. 2016), especially considering it is a relatively small cell growing at higher temperature than commonly used (24°C vs. 20°C). It might be expected that the growth rate of *Florenciella* under autotrophic conditions would be relatively slow compared to pure autotrophs, because of the added cost of maintaining phagotrophy. However, this tradeoff may be consequential only when the supply of light or nutrients is low, because reduced investment in photosynthesis or nutrient uptake will more strongly limit growth rate in those cases. The observation that *Florenciella* does not significantly graze at high nutrient concentrations may mean that the cost of having a generalist trophic strategy is mitigated by this plasticity. When *Florenciella* was fed ample *Synechococcus*, its growth was faster than under purely autotrophic conditions (Fig. 4). This could be attributable to an increase in energy supply from prey catabolism, supplementing the energy obtained from photosynthesis, or might result from a lower energetic cost of anabolism compared to synthesis from inorganic nutrients. When compared to heterotrophic nanoflagellates, a maximum growth rate of 3 d^{-1} is typical (Hansen et al. 1997), implying that under conditions of ample light and prey a mixotrophic strategy is not costly compared to a heterotrophic strategy. However, *Florenciella* cannot grow in the dark when fed prey, which has been observed for a number of mixotrophic grazers (Hansen 2011). Its ability to compete against heterotrophic grazers may therefore depend on receiving sufficient irradiance.

Grazing behavior in response to nutrient limitation and time of day

We found that nitrogen or phosphorus limitation induces substantially faster grazing rates in *Florenciella*, which also has been found among other mixotrophs, for example, haptophytes (Chan et al. 2019) and chlorophytes (Anderson et al. 2018). Such plasticity may have been selected for in mixotrophs and be a widespread adaptation, as similar patterns have been found in phylogenetically diverse taxa.

Ribalet et al. (2015) estimated *Prochlorococcus* division and mortality rates in situ in the NPSG using a size-structured population growth model. They predicted elevated *Prochlorococcus* mortality at night, peaking around midnight, and lower mortality during the day, with negligible rates near noon. Although we found evidence for modest diel variation in *Florenciella* ingestion, the timing and magnitude is inconsistent with the results of Ribalet et al. (2015), as we observed that ingestion rate increased during the day and peaked in the late afternoon or early evening (Fig. 7). If *Prochlorococcus* mortality rates peak around midnight, this may be driven by other grazers or by viruses. While mechanisms underlying the diel rhythmicity of phagotrophic activities are not entirely understood (Arias et al. 2019), some studies have suggested mixotrophic grazing is positively tied to photosynthetic activities aided by light (Stoecker 1998), such that more nutrients (prey) are required to keep up with the high photosynthesis rates during later times of the day.

Grazing on different bacterial taxa

The higher clearance rates of *Florenciella* when ingesting *Synechococcus* relative to *Prochlorococcus* is consistent with studies where these prey types were grazed by heterotrophic flagellates (Christaki et al. 2002). It is possible that *Florenciella* actively rejected *Prochlorococcus* in favor of *Synechococcus*, but the differences in clearance rate were also observed in the single-prey experiments, at least when initial prey density is $< 10^6$ cells mL^{-1} (Fig. 5c). This suggests that differences resulted from encounter rate or capture efficiency, perhaps attributable to differences in cell size or surface properties (Monger et al. 1999). The higher relative ingestion of 1.0 μm relative to 0.5 μm beads when present at the same concentration (Fig. 2) is consistent with size being the explanation for the higher rates of ingestion of *Synechococcus* vs. *Prochlorococcus*. However, the much lower uptake overall for polystyrene microspheres compared to cells also illustrates that surface properties are important, and the use of these types of synthetic beads can lead to significant underestimates of prey uptake capabilities (Nygaard et al. 1988).

The grazing rates of *Florenciella* on two heterotrophic bacterial strains, although derived using natural prey, may not be representative of in situ rates of grazing on heterotrophic bacteria. The strains used were isolated from cultures of *Florenciella*, which could have favored grazing-resistant strains. These larger, copiotrophic isolates are also not representative of the most common types of bacteria in the NPSG, which include small, slow-growing members of the SAR11 clade (Eiler et al. 2009). Nevertheless, *Marinobacter*, which was similar to *Prochlorococcus* in size, was also grazed at a comparable rate. In contrast, the rod-shaped *Rhodobacteraceae* isolate was ingested very poorly despite being only slightly longer (1.4 μm) than the diameter of *Synechococcus* (1.22 μm). This bacterium may be just over the maximum dimension that can be handled by *Florenciella*, or it may have other properties that deter capture or ingestion (Pernthaler 2005).

Plasticity of grazing in response to prey density

One of the unexpected findings of this study is that the grazing parameters I_{max} and C_{max} are negatively correlated with each other, and they correlate with the initial prey density used during the experiments, such that *Florenciella* experiencing lower prey density tend to exhibit a higher C_{max} and a lower I_{max}. These relationships are distinct from the fact that clearance rate tends to decline as prey density increases (Frost 1972), because they pertain to the maximum clearance rate, which is the initial slope of the ingestion rate vs. prey density curve. These patterns suggest that *Florenciella* can adaptively acclimate its grazing behavior according to prey availability. It may also be adaptive to reduce swimming speed (and thereby C_{max}) as prey concentration increases (Kiørboe 2011), because greater swimming speed increases contact with predators and viruses (Talmy et al. 2019). Plasticity of these traits may be advantageous if *Florenciella* experience substantial temporal variation in prey concentration, which could occur if they forage on dilute, free-living bacteria as well as dense aggregations that occur on detrital particles (Stocker et al. 2008). These results suggest that estimates of flagellate functional responses may be sensitive to the recent history of the cultures, and that the acclimated functional response under relatively constant conditions may differ from the instantaneous functional response (Fig. 5f), analogous to the difference between instantaneous and acclimated photosynthesis-irradiance curves (Givnish 2002).

Ecological implications of grazing by *Florenciella*

Using the grazing results for *Florenciella* and estimates of in situ nanoflagellates and prey concentrations, we can roughly estimate the contribution to cyanobacterial mortality in the NPSG, an environment with persistently depleted surface nutrients and relatively stable microbial distributions throughout the year (Karl and Church 2014). Pigmented nanoflagellates in the upper euphotic zone at Sta. ALOHA are typically $\sim 2 \times 10^3$ cells mL^{-1} (Calbet et al. 2001), dominated by cells < 3 μm, many of which may be mixotrophic based on results from another oligotrophic habitat (Hartmann et al. 2012). Amplicon sequencing (18S rDNA) suggests that *Florenciella* accounts for up to $\sim$ 10% of eukaryotes ≤ 3 μm and is one of the more abundant groups in the NPSG (Rii et al. 2018). Multiplying the maximum clearance rate (volume *Florenciella*$^{-1}$ time^{-1}) by *Florenciella* abundance (*Florenciella* volume^{-1}) yields a specific rate of mortality

imposed on a prey population (time^{-1}). Using C_{max} values of 1.5 nL *Florenciella*$^{-1}$ h^{-1} for *Prochlorococcus* or bacteria as prey, and 5 nL *Florenciella* $^{-1}$ h^{-1} for *Synechococcus* (Fig. 5), we predict that *Florenciella* consumes up to 0.7% of *Prochlorococcus* and bacteria and 2.4% of *Synechococcus* standing stock daily, or 1.3%, 0.7%, and 2.4% of the daily production assuming their respective growth rates are about 0.55 (Liu et al. 1997), 0.97 (Jones et al. 1996), and 1.0 d^{-1} (Liu et al. 1998).

If all mixotrophic nanoflagellates were similar to *Florenciella* and all the pigmented eukaryotes at Station ALOHA were mixotrophs, they collectively would consume 13% of *Prochlorococcus*, 7% of heterotrophic bacteria, and 24% of *Synechococcus* produced per day. In situ estimates of nanoflagellate grazing on bacteria are variable, yet they are generally in agreement with our study. Hartmann et al. (2012) used radiolabeled bacterial communities and found that pigmented flagellates (< 3 μm) consumed $\sim 2 \times 10^3$ bacteria mL^{-1} h^{-1}, or $\sim$ 10–15% of the prey population daily in the oligotrophic Atlantic; unpigmented flagellates consumed roughly half as much.

We can also ask what in situ growth rates of *Florenciella* are feasible based on the grazing parameters we have estimated. Assuming that the respective *Prochlorococcus* and bacteria concentrations are 2×10^5 and 5×10^5 cells mL^{-1}, and their N quotas are $\sim$ 10 fg N (Baer et al. 2017) and 2 fg N cell^{-1} (synthesized in White et al. 2019), and the N quota of *Florenciella* is 475 fg N cell^{-1}, then *Florenciella* would achieve a N-specific N ingestion rate of 0.2 d^{-1}. Uptake kinetics of dissolved N by *Florenciella* are unknown, but a specific uptake affinity for dissolved inorganic N of $\sim$ 20 L μmol N^{-1} d^{-1} is reasonable based on allometric scaling relationships (Edwards et al. 2012). Assuming DIN at Station ALOHA is $\sim$ 0.01 μM, N-specific N uptake would be 0.2 d^{-1}, equal to the N derived from prey and yielding a total N-limited growth rate of 0.4 d^{-1}. This is similar to bulk estimates of phytoplankton growth rates in oligotrophic waters (Marañón et al. 2014).

Conclusion

In sum, our results suggest that mixotrophy is an effective strategy for nutrient acquisition by *Florenciella*, with phagotrophic abilities that are highly plastic and somewhat lower than those of pure heterotrophs. If open ocean mixotrophic nanoflagellates grazing capabilities are generally comparable to *Florenciella*, then their overall contribution to mortality of *Prochlorococcus* could be significant, but alone would not balance in situ growth rates. Efficient retention of prey N by *Florenciella* may reduce nutrient availability for autotrophs, and energy derived from photosynthesis may allow them to compete strongly for prey, even if heterotrophic nanoflagellates have greater maximum clearance rates. Understanding the role of flagellates in microbial food webs will require additional isolation and experimentation similar to this study, because different taxa and genotypes within taxa may vary substantially in their grazing ability, with important consequences for the control of prey populations, nutrient cycling, and productivity.

References

Anderson, R., S. Charvet, and P. J. Hansen. 2018. Mixotrophy in chlorophytes and haptophytes—effect of irradiance, macronutrient, micronutrient and vitamin limitation. Front. Microbiol. **9**: 1704. doi:10.3389/fmicb.2018.01704

Arias, A., E. Saiz, and A. Calbet. 2019. Towards an understanding of diel feeding rhythms in marine protists: Consequences of light manipulation. Microb. Ecol. **79**: 64–72. doi:10.1007/s00248-019-01390-y

Baer, S. E., M. W. Lomas, K. X. Terpis, C. Mouginot, and A. C. Martiny. 2017. Stoichiometry of *Prochlorococcus*, *Synechococcus*, and small eukaryotic populations in the western North Atlantic Ocean. Environ. Microbiol. **19**: 1568–1583.

Bolker, B. M. 2017. R Development Core Team. Package 'bbmle'. Tools for general maximum likelihood estimation. CRAN Repository, version1.0.17. Available from http://cran.rproject.org/web/packages/bbmle/index.html

Calbet, A., M. R. Landry, and S. Nunnery. 2001. Bacteria-flagellate interactions in the microbial food web of the oligotrophic subtropical North Pacific. Aquat. Microb. Ecol. **23**: 283–292.

Caron, D. A. 2001. Protistan herbivory and bacterivory, p. 289–315. *In* J. H. Paul [ed.], Marine microbiology. Academic.

Chan, Y. F., K. P. Chiang, Y. Ku, and G. C. Gong. 2019. Abiotic and biotic factors affecting the ingestion rates of mixotrophic nanoflagellates (Haptophyta). Microb. Ecol. **77**: 607–615.

Chisholm, S. W. 2012. Unveiling *Prochlorococcus*: The life and times of the ocean's smallest photosynthetic cell, p. 165–171. *In* R. Kolter and S. Maloy [eds.], Microbes and evolution: The world that Darwin never saw. ASM Press.

Christaki, U., C. Courties, H. Karayanni, A. Giannakourou, C. Maravelias, K. A. Kormas, and P. Lebaron. 2002. Dynamic characteristics of *Prochlorococcus* and *Synechococcus* consumption by bacterivorous nanoflagellates. Microb. Ecol. **43**: 341–352.

Edwards, K. F. 2019. Mixotrophy in nanoflagellates across environmental gradients in the ocean. Proc. Natl. Acad. Sci. USA **116**: 6211–6220.

Edwards, K. F., M. K. Thomas, C. A. Klausmeier, and E. Litchman. 2012. Allometric scaling and taxonomic variation in nutrient utilization traits and maximum growth rate of phytoplankton. Limnol. Oceanogr. **57**: 554–566.

Eikrem, W., K. Romari, M. Latasa, F. L. Gall, J. Throndsen, and D. Vaulot. 2004. *Florenciella parvula* gen. et sp. nov. (Dictyochophyceae, Heterokontophyta), a small flagellate isolated from the English Channel. Phycologia **43**: 658–668.

Eiler, A., D. H. Hayakawa, M. J. Church, D. M. Karl, and M. S. Rappé. 2009. Dynamics of the SAR11 bacterioplankton

lineage in relation to environmental conditions in the oligotrophic North Pacific subtropical gyre. Environ. Microbiol. **11**: 2291–2300.

Fischer, R., H. A. Giebel, H. Hillebrand, and R. Ptacnik. 2017. Importance of mixotrophic bacterivory can be predicted by light and loss rates. Oikos **126**: 713–722.

Frias-Lopez, J., A. Thompson, J. Waldbauer, and S. W. Chisholm. 2009. Use of stable isotope-labelled cells to identify active grazers of picocyanobacteria in ocean surface waters. Environ. Microbiol. **11**: 512–525.

Frost, B. W. 1972. Effects of size and concentration of food particles on the feeding behavior of the marine planktonic copepod *Calanus pacificus*. Limnol. Oceangr. **17**: 805–815.

Gast, R. J., S. A. Fay, and R. W. Sanders. 2018. Mixotrophic activity and diversity of Antarctic marine protists in austral summer. Front. Mar. Sci. **5**: 13. doi:10.3389/fmars.2018.00013

Gerea, M., C. Queimaliños, and F. Unrein. 2019. Grazing impact and prey selectivity of picoplanktonic cells by mixotrophic flagellates in oligotrophic lakes. Hydrobiologia **831**: 5–21.

Givnish, T. J. 2002. Ecological constraints on the evolution of plasticity in plants. Evol. Ecol. **16**: 213–242.

Hansen, P. J., P. K. Bjørnsen, and B. W. Hansen. 1997. Zooplankton grazing and growth: Scaling within the 2–2000 µm body size range. Limnol. Oceanogr. **42**: 687–704.

Hansen, P. J. 2011. The role of photosynthesis and food uptake for the growth of marine mixotrophic dinoflagellates. J. Euk. Microbiol. **58**: 203–214.

Hartmann, M., C. Grob, G. A. Tarran, A. P. Martin, P. H. Burkill, D. J. Scanlan, and M. V. Zubkov. 2012. Mixotrophic basis of Atlantic oligotrophic ecosystems. Proc. Natl. Acad. Sci. USA **109**: 5756–5760.

Jeong, H., and others. 2005. Feeding by red–tide dinoflagellates on the cyanobacterium *Synechococcus*. Aquat. Microb. Ecol. **41**: 131–143.

Jones, D. R., D. M. Karl, and E. A. Laws. 1996. Growth rates and production of heterotrophic bacteria and phytoplankton in the North Pacific subtropical gyre. Deep-Sea Res. Pt. I **43**: 1567–1580.

Jones, R. I. 2000. Mixotrophy in planktonic protists: An overview. Freshwater Biol. **45**: 219–226.

Karl, D. M., and M. J. Church. 2014. Microbial oceanography and the Hawaii Ocean time-series programme. Nat. Rev. Microbiol. **12**: 699–713.

Keller, M. D., R. C. Selvin, W. Claus, and R. R. L. Guillard. 1987. Media for the culture of oceanic ultraphytoplankton. J. Phycol. **23**: 633–638.

Kiørboe, T. 2011. How zooplankton feed: Mechanisms, traits and trade-offs. Biol. Rev. **86**: 311–339.

Leakey, R. J. G., S. A. Wilks, and A. W. A. Murray. 1994. Can cytochalasin B be used as an inhibitor of feeding in grazing experiments on ciliates? Eur. J. Protistol. **30**: 309–315. doi:10.1016/S0932-4739(11)80077-5

Legrand, C., N. Johansson, G. Johnsen, K. Y. Borsheim, and E. Granéli. 2001. Phagotrophy and toxicity variation in the mixotrophic *Prymnesium patelliferum* Haptophyceae. Limnol. Oceanogr. **46**: 1208–1214.

Lindehoff, E., E. Granéli, and P. M. Glibert. 2010. Influence of prey and nutritional status on the rate of nitrogen uptake by *Prymnesium parvum* (haptophyte). J. Am. Water Resour. As. **46**: 121–132.

Liu, H., L. Campbell, M. R. Landry, H. A. Nolla, S. L. Brown, and J. Constantinou. 1998. *Prochlorococcus* and *Synechococcus* growth rates and contributions to production in the Arabian Sea during the 1995 southwest and northeast monsoons. Deep-Sea Res. Pt. II **45**: 2327–2352.

Liu, H., H. A. Nolla, and L. Campbell. 1997. *Prochlorococcus* growth rate and contribution to primary production in the equatorial and subtropical North Pacific Ocean. Aquat. Microb. Ecol. **12**: 39–47.

Marañón, E., P. Cermeño, M. Huete-Ortega, D. C. López-Sandoval, B. Mouriño-Carballido, and T. Rodríguez-Ramos. 2014. Resource supply overrides temperature as a controlling factor of marine phytoplankton growth. PLoS One **9**: e99312. doi:10.1371/journal.pone.0099312

Marie, D., F. Rigaut-Jalabert, and D. Vaulot. 2014. An improved protocol for flow cytometry analysis of phytoplankton cultures and natural samples. Cytom. Part A **85**: 962–968. doi:10.1002/cyto.a.22517

McKie-Krisberg, Z. M., R. J. Gast, and R. W. Sanders. 2014. Physiological responses of three species of Antarctic mixotrophic phytoflagellates to changes in light and dissolved nutrients. Microb. Ecol. **70**: 21–29. doi:10.1007/s00248-014-0543-x

Monger, B. C., M. R. Landry, and S. L. Brown. 1999. Feeding selection of heterotrophic marine nanoflagellates based on the surface hydrophobicity of their picoplankton prey. Limnol. Oceanogr. **44**: 1917–1927.

Moore, L. R., and others. 2007. Culturing the marine cyanobacterium *Prochlorococcus*. Limnol. Oceanogr.: Methods **5**: 353–362.

Nygaard, K., K. Y. Børsheim, and T. F. Thingstad. 1988. Grazing rates on bacteria by marine heterotrophic microflagellates compared to uptake rates of bacterial-sized monodisperse fluorescent latex beads. Mar. Ecol. Prog. Ser. **44**: 159–165.

Partensky, F., J. Blanchot, and D. Vaulot. 1999. Differential distribution and ecology of *Prochlorococcus* and *Synechococcus* in oceanic waters: A review. Bull. Inst. Oceanogr. Monaco **19**: 457–476.

Pernthaler, J. 2005. Predation on prokaryotes in the water column and its ecological implications. Nat. Rev. Microbiol. **3**: 537–546.

Ribalet, F., and others. 2015. Light–driven synchrony of *Prochlorococcus* growth and mortality in the subtropical Pacific gyre. Proc. Natl. Acad. Sci. USA **112**: 8008–8012.

Rii, Y. M., R. R. Bidigare, and M. J. Church. 2018. Differential responses of eukaryotic phytoplankton to nitrogenous nutrients in the North Pacific Subtropical Gyre. Front. Mar. Sci. **5**: 92. doi:10.3389/fmars.2018.00092

Sanders, R. W. 1991. Mixotrophic protists in marine and freshwater ecosystems. J. Protozool. **38**: 76–81.

Sanders, R. W., U. G. Berninger, E. L. Lim, P. F. Kemp, and D. A. Caron. 2000. Heterotrophic and mixotrophic nanoplankton predation on picoplankton in the Sargasso Sea and on Georges Bank. Mar. Ecol. Prog. Ser. **192**: 103–118.

Sandhu, S. K., A. Y. Morozov, A. Mitra, and K. Flynn. 2019. Exploring nonlinear functional responses of zooplankton grazers in dilution experiments via optimization techniques. Limnol. Oceanogr. **64**: 774–784.

Sherr, B. F., E. B. Sherr, and R. D. Fallon. 1987. Use of monodispersed, fluorescently labeled bacteria to estimate in situ protozoan bacterivory. Appl. Environ. Microbiol. **53**: 958–965.

Soetaert, K. E., T. Petzoldt, and R. W. Setzer. 2010. Solving differential equations in R: Package deSolve. J. Stat. Softw. **33**: 1–25. doi:10.18637/jss.v033.i09

Stoecker, D. K. 1998. Conceptual models of mixotrophy in planktonic protists and some ecological and evolutionary implications. Europ. J. Protistol. **34**: 281–290.

Stoecker, D. K., P. J. Hansen, D. A. Caron, and A. Mitra. 2017. Mixotrophy in the marine plankton. Ann. Rev. Mar. Sci. **9**: 311–335.

Stocker, R., J. R. Seymour, A. Samadani, D. E. Hunt, and M. F. Polz. 2008. Rapid chemotactic response enables marine bacteria to exploit ephemeral microscale nutrient patches. Proc. Natl. Acad. Sci. USA **105**: 4209–4214.

Talmy, D., S. J. Beckett, A. B. Zhang, D. A. Taniguchi, J. S. Weitz, and M. J. Follows. 2019. Contrasting controls on microzooplankton grazing and viral infection of microbial prey. Front. Mar. Sci. **6**: 182. doi:10.3389/fmars.2019.00182

Thomas, M. K., C. T. Kremer, and E. Litchman. 2016. Environment and evolutionary history determine the global biogeography of phytoplankton temperature traits. Glob. Ecol. Biogeogr. **25**: 75–86.

Ward, B. A., E. Marañón, B. Sauterey, J. Rault, and D. Claessen. 2017. The size dependence of phytoplankton growth rates: A trade-off between nutrient uptake and metabolism. Am. Nat. **189**: 170–177.

Weisse, T., R. Anderson, H. Arndt, A. Calbet, P. J. Hansen, and D. J. Montagnes. 2016. Functional ecology of aquatic phagotrophic protists—concepts, limitations and perspectives. Eur. J. Protistol. **55**: 50–74.

White, A. E., S. J. Giovannoni, Y. L. Zhao, K. Vergin, and C. A. Carlson. 2019. Elemental content and stoichiometry of SAR11 chemoheterotrophic marine bacteria. Limnol. Oceanogr.: Lett. **4**: 44–51.

Wood, S. N. 2011. Fast stable restricted maximum likelihood and marginal likelihood estimation of semiparametric generalized linear models. J. R. Stat. Soc. Series B. Stat. Methodol. **73**: 3–36. doi:10.1111/j.1467-9868.2010.00749.x

Wood, S., and S. Fabian. 2017. Package 'gamm4'. Am. Stat. **45**: 339 CRAN Repository, https://CRAN.R-project.org/package=gamm4

Worden, A. Z., M. J. Follows, S. J. Giovannoni, S. Wilken, A. E. Zimmerman, and P. J. Keeling. 2015. Rethinking the marine carbon cycle: Factoring in the multifarious lifestyles of microbes. Science **347**: 735–747.

Acknowledgments

This work was supported by National Science Foundation awards OCE 15-59356 (to G.F.S, K.F.E., and K.E.S.) and RII Track-2 FEC 1736030 (to G.F.S. and K.F.E.), and a Simons Foundation Investigator Award in Marine Microbial Ecology and Evolution (to K.F.E.). We thank the personnel in the Hawai'i Ocean Time-series program (NSF award 12-60164) for assistance with collecting water samples. We thank Dr. Sallie W. Chisholm (Massachusetts Institute of Technology) for providing the *Prochlorococcus* and *Synechococcus* strains. We are also grateful to Tina M. Weatherby at the Pacific Biosciences Research Center Biological Electron Microscope Facility at University of Hawai'i at Mānoa (UHM) for her assistance with imaging and to the editor and two anonymous reviewers for thoughtful comments that improved the manuscript. Acquisition of the confocal microscope was made possible by support from NSF (MRI 18-28262) and matching funds from the Office of the Vice Chancellor for Research at UHM. The transmission electron microscope was acquired with funding from NSF (DBI 10-40548).

Conflict of Interest

All authors declare that they have no conflicts of interest related to this work.

Submitted 27 November 2019
Revised 24 March 2020
Accepted 25 July 2020

Associate editor: Birte Matthiessen